

Crystal Structure and Banded Spherulite of Poly(trimethylene terephthalate)

Rong-Ming Ho*

Department of Chemical Engineering, National Chung Hsing University, Taichung 40227, Taiwan, R.O.C.

Kae-Zen Ke and Ming Chen

Institute of Materials Science and Engineering, National Sun Yet-Sen University, Kaohsiung 80424, Taiwan, R.O.C.

Received February 4, 2000; Revised Manuscript Received June 26, 2000

ABSTRACT: Developments of single crystal ED patterns in melt-crystallized poly(trimethylene terephthalate) (PTT) have been successfully achieved. Five different zonal electron diffraction patterns containing a total of 14 independent reflections were obtained. The PTT structure under strain-free conditions was identified as a triclinic structure with $a = 4.5$ Å, $b = 6.3$ Å, $c = 18.2$ Å, $\alpha = 97.5^\circ$, $\beta = 91.4^\circ$, and $\gamma = 111.7^\circ$ with a calculated density of 1.44 g/cm³. On the basis of the corresponding reflections in ED patterns, each significant diffraction peak in wide-angle X-ray diffraction powder pattern was identified and indexed. A much more precise determination of the unit cell parameters has been thus achieved. They are $a = 4.53$ Å, $b = 6.20$ Å, $c = 18.70$ Å, $\alpha = 97.6^\circ$, $\beta = 93.2^\circ$, and $\gamma = 110.1^\circ$. Unlike poly(butylene terephthalate), structure deformation has not been found in PTT fibers after removal of the extension. This specific feature may explain the better performance in resilience recovery for PTT as compared to PET and PBT. Banded spherulite with negative birefringence has been observed in PTT under polarized light microscopy. The formation of banded spherulites is attributed to lamellar twisting. The twisting mechanism was evidenced by the observations of wavylike morphology from reflected light microscopy and transmission electron microscopy. The geometry of crystal lamellae has been identified according to lamellar morphology and its correlated single-crystal ED patterns. The PTT lamellae grow from the basal plane consisting of a and b axes. In connection with the observed morphology, we suggest that the lamellar twisting is attributed to the tilted chain stems which are nonorthogonal to fold surface. The nonorthogonal geometry results from the growth of PTT lamellae with triclinic structure where internal stress is gradually accumulated so as to drive the crystal twist along the radial direction of spherulite.

Introduction

Poly(trimethylene terephthalate) (PTT) is one member of the terephthalic polyesters, the most common substances used in engineering thermoplastics. More recently, PTTs have drawn attention for their applications in textile industry due to a great reduction in the manufacturing cost of 1,3-propanediol, the monomer used for PTT synthesis.¹ Although other members of terephthalic polyesters such as poly(ethylene terephthalate) (PET) and poly(butylene terephthalate) (PBT) have been intensively studied, there were only a few studies performed on PTT in the past. The crystal structure of PTT has been mainly examined by wide-angle X-ray diffraction (WAXD) of drawn fibers.^{2–4} Although single crystals of PTT for electron diffraction (ED) experiments have also been successfully grown from solution,⁴ only a single [001] zonal diffraction was obtained, and a detailed analysis of ED experiments has not yet been performed. In the family of terephthalic polyesters, it has been justified that the structure parameters may vary with mechanical deformation applied upon samples.^{3,5–11} In particular, a structure transformation from the α form to the β form for PBT has been found after the deformation.^{3,9–11} Significant changes in unit cell parameters occurred after the transformation. A similar transformation has also been

found in poly(pentamethylene terephthalate).^{12,13} It is still in debate whether the transformation reverts or the transformed structure remains due to residual stresses after the removal of deformation. It will be difficult to justify whether fiber samples return to their stable structure even though they are able to relax through thermal annealing. To unify the determined structure unambiguously, it is necessary to have strain-free crystals for the structure examination. Single crystal experiments are the solution to obtain the structure parameters of stable crystals. Developments of large single lamellae from solution have helped to solve the problems, but the population of grown lamellae is minor due to the requirement of dilution for the growth of large crystals. Melt crystallization was thus carried out in this study in order to examine the crystal structure and morphology of PTT in detail. A great population of large lamellae has been successfully grown in this study. To the best of our knowledge, this is the first time that large enough lamellae of terephthalic polyesters have been grown from the melt for single-crystal ED experiments.

The morphology of banded spherulites under transmitted polarized light microscopy (PLM) is commonly observed in crystalline polymers. It is generally believed that the formation of banded spherulite is attributed to lamellar twisting about the direction of radial growth.^{14–19} Currently, the mechanisms of lamellar twisting within spherulite are referred to two models. They are interlamellar^{20–24} and intralamellar ori-

* To whom all correspondence should be addressed. Telephone: 886-4-2857471. Fax: 886-4-2854734. E-mail: rmho@dragon.nchu.edu.tw.

gins.^{14–16,25–29} For interlamellar origin, equally spaced screw dislocations along the radial growth direction of the lamellae are formed so as to give rise to the twisting of molecular stems at the lamellar level. The overall twist to the radially growing lamellae is thus initiated by this sequence of transverse screw dislocations with the same sign so that the banding extinction pattern is observed under PLM. The diverse translation of the molecular stems at screw dislocations is raised by the results for disordered cilia associated with the fold surfaces of neighboring lamellae. Namely, it is an interlamellar origin to the lamellar geometry. The model was originally proposed by Schultz and Kinloch²⁰ and then modified by Bassett and co-workers in great detail.^{21–24} The asymmetric development around screw dislocations suggests a solution to the problem of the formation of banded spherulites.^{24,30}

For intralamellar origin, regularly twisted molecular stems are cooperatively accommodated in continuously twisted helical lamellae without the presence of screw dislocations. The twisting is attributed mainly to the influence of the surface stresses resulting from the asymmetry of lamellar geometry. The model was initially proposed by Keller²⁵ and has been developed intensively by Keith and Padden.^{15–16,27} The fold staggering might cause the chain stems to be nonorthogonal to the fold surfaces so as to generate unequal stresses at opposite fold surfaces. The unequal stresses yield bending moments upon lamellae that finally results in the twisting of the lamellae. In other words, the twisting is attributed to an intralamellar origin to the lamellar geometry.

These two twisting mechanisms have been well applied to various crystalline polymers having banded extinction. However, more than one type of molecular arrangement corresponding to the lamellar geometry has been proposed to describe the twisting origins. Detailed descriptions of the orientation relationships between the twisted molecular arrangement and the organization of a lamellar geometry have only been given in a few crystalline polymers. Recently, a twisted helical geometry has also been found in a series of chiral liquid crystalline polymers where the helical geometry is identified as a double-twisted helix.^{31,32} The majority of previous studies in the issue of banded spherulite origins reported the results of etching or staining morphology. In this study, typical banded extinction has been found in melt-crystallized spherulites of PTT under transmitted PLM. Direct observation of the banded spherulites has been performed under TEM and found that the spherulites comprised large lamellae at which the lamellar geometry was established by ED experiments. Combined with morphological observation and ED results, a detailed investigation of the formation of banded extinction was achieved. A geometric model is thus proposed to describe the lamellar twisting in banded spherulites of terephthalic polyesters.

Materials

Developmental grade PTT was synthesized by polyesterification of terephthalic acid and 1,3-propanediol. The number-average molecular weight of the samples is 28 250 and the polydispersity is 2.5.

PTT thin films with thickness in the range of micrometers for PLM and of 10 nm for TEM observation, respectively, were prepared by casting a 0.2–1% (w/w) phenol and 1,1,2,2-tetrachloroethane solution onto glass slides. The ratio of phenol to 1,1,2,2-tetrachloroethane in solution was $\frac{3}{2}$ by weight. For

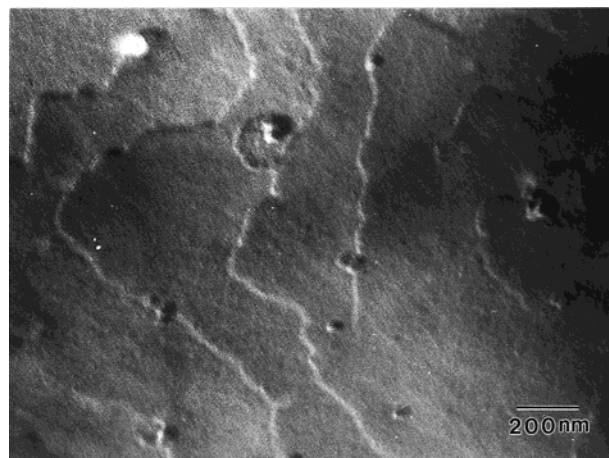


Figure 1. TEM observation of PTT single lamellar morphology crystallized at 225 °C from the melt.

TEM observation, the glass slides were coated with carbon before casting. PTT samples were heated to ca. 30 °C above their highest melting temperature for several minutes in a dry argon atmosphere and then rapidly cooled to a preset temperature for melt crystallization. After crystallization at different temperatures, the films were quenched into liquid nitrogen and then observed under PLM at room temperature. For TEM observation, the quenched samples were shadowed by Pt and coated with carbon again. After shadowing, the PTT films were stripped and floated onto the water surface and then recovered using copper grids.

For the WAXD study, the same crystallization conditions for PTT bulk samples were carried out. Filaments of PTT fibers were spun from the melt and extruded at temperatures above the glass transition temperature. After extrusion, the filaments were immediately cooled by cold air.

Experimental Section

PTT crystal morphology and ED patterns were observed via a JEOL (JEM-1200x) TEM using an accelerating voltage of 120 kV. Bright field images were obtained by the mass-thickness contrast from shadowing. A tilting stage was used in the ED experiments to determine the three-dimensional crystalline lattice. Calibration of the electron diffraction spacing was carried out using Au and TiCl₃ (d spacing < 3.84 Å, the largest spacing for TiCl₃). Spacing values larger than 3.84 Å were calibrated by doubling the d spacings of these reflections.

The spherulitic morphology of PTT samples was observed via a PLM instrument (Olympus BX60) installed with a DP10 digital camera. Light sources of reflected and transmitted modes were both used to obtain optical images.

A Siemens D5000 1.2 kW tube X-ray generator (Cu K α radiation) with a diffractometer was used for WAXD powder experiments. The scanning 2θ angle ranged between 5 and 40° with a step scanning of 0.05° for 3 s. The diffraction peak positions and widths observed from WAXD experiments were carefully calibrated with silicon crystals with known crystal size. Fiber WAXD patterns were obtained using a flat-plate vacuum camera (Enraf-Nonius 582 D60) attached to a Siemens tube X-ray generator. The calibration was also carried out by the reflections of silicon crystals.

Results

Structure of Melt-Crystallized PTT. Large single lamellar crystals with micrometer size and smooth surface have been successfully grown from the melt as shown in Figure 1. The corresponding different zonal ED patterns of single lamellar crystal were thus obtained through tilting experiments under TEM. They are [001], [221], [201], [301], and [321] zone ED patterns

as shown in Figure 2, parts a–e, respectively. From these patterns fourteen independent reflections were identified. Unit cell parameters of $a = 4.5 \text{ \AA}$, $b = 6.3 \text{ \AA}$, $c = 18.2 \text{ \AA}$, $\alpha = 97.5^\circ$, $\beta = 91.4^\circ$, and $\gamma = 111.7^\circ$, with a relative deviation less than 0.01, were calculated by least-squares refinement based on the plane spacing. The corresponding interplanar angles were calculated in accordance with the determined triclinic unit cell. Comparing with the observed interplanar angles in ED patterns, the calculated results gave adequately good agreement with the experimental measurements (see Figure 2 and Table 2). The density of the crystal structure was calculated as 1.44 g/cm^3 . Furthermore, we have found that the majority of observed ED patterns exists certain reflections, such as (101) in [001] zone, (113) in [201] zone, and (102) in [321] zone, which cannot be assigned according to the zone law of diffraction. For example, it is not possible to find a consistent zone axis for the coexistence of (101), (100), and (010) in the same ED pattern. These out-of-zone reflections are all distinguished from l of Miller indices of neighboring in-zone reflections. We speculate that the appearance of abnormal reflections is attributed to the lamellar tilting during growth. This hypothesis is consistent with proposed mechanism for the formation of banded morphology (see discussion section in detail).

Figure 3 shows the WAXD powder patterns of PTT crystallized at 225°C for more than 20 h from the melt. On the basis of plane spacing and intensity of reflections in ED patterns, each significant diffraction peak in WAXD powder pattern was identified and indexed (Figure 3). After the identification of corresponding reflections, set of unit cell parameters with superior precision was thus obtained by least-squares refinement. They are $a = 4.53 \text{ \AA}$, $b = 6.20 \text{ \AA}$, $c = 18.70 \text{ \AA}$, $\alpha = 97.6^\circ$, $\beta = 93.2^\circ$, and $\gamma = 110.1^\circ$, with a relative deviation around 0.01 (see Table 1). For PTT molecules, there are three methylene units between terephthaloyl moieties, and thus there cannot be any center of symmetry in the middle of the trimethylene part of the chain. The packing of molecular chains possesses a 2/1 helical structure due to the odd number of methylene groups.⁴ It is a two-chain triclinic structure and its space group is $P\bar{1}$. The density of the crystal structure was calculated as 1.408 g/cm^3 .

Structure of PTT Fibers. As described in the Introduction, the unit cell dimensions, particularly in the c axis, for terephthalic polyesters may vary with draw ratio and subsequent annealing temperature as well as annealing time. To examine whether the unit cell dimensions are affected by drawing or not, filaments of PTT fiber were prepared through spinning experiments. After drawing, PTT fibers without any further annealing were examined by using WAXD (Figure 4). Although the reflections of fiber pattern are quite weak due to the lack of crystallinity, a strong (002) reflection accompanying diffused (010), (012), and (113) reflections can be observed. The c axis dimension was thus determined as 18.74 \AA .

Banded Spherulites of Melt Crystallized PTT. The appearance of PTT samples, crystallized from the melt at different crystallization temperatures, between crossed polaroids are shown in Figure 5, parts a–d. These melt-crystallized PTT thin films with free surface formed well-developed, two-dimensional spherulites. They revealed a dark Maltese cross along the vibrational directions of polarizer and analyzer. The optical behav-

ior of these spherulites exhibited a typical negative birefringence (i.e., the first and third quadrants of spherulite appear yellow but the second and fourth quadrants appear blue) while the samples were observed under PLM with the birefringence enhancement of a gypsum plate. In addition to these usual observations for polymeric materials, a system of dark concentric rings could be seen while the samples were crystallized at higher crystallization temperature. These observed ringed images are similar to the morphology of banded spherulite, which is generally observed in certain polymeric materials. As observed, the appearance of the banded spherulite in PTT was strongly dependent upon the level of crystallization temperature; the separation of these bands decreased with the reducing of crystallization temperature. At lower temperatures of crystallization, the banded morphology disappeared and exhibited regular spherulitic image (Figure 5, parts a and b). A temperature range (above 195°C) for the formation of banded spherulite in a PTT thin film was thus determined based on PLM observations. It can be seen further that these rings may be circles or spirals if followed to the center. The spiral and circular morphology were clearly identified while the spherulite was observed by reflected light microscopy (Figure 6). Corresponding to the morphological observations by light microscopy, PTT thin film samples were viewed by TEM (Figure 7, parts a–c). At lower crystallization temperature (below 200°C), TEM micrographs (as an example, shown in Figure 7a) exhibit ordinary spherulitic morphology comprising of lamellar fibrils that are radially branching out. Comparing with the low temperature morphology, the PTT spherulites grown at higher crystallization temperature exhibit distinctive images. These lamellar fibrils spirally protrude from the center of spherulites (Figure 7, parts b and c). The spiral morphologies may occur in both clockwise and counterclockwise directions. These two directions of spiral twists were found to occur with equal probability in the observed banded spherulites. This result is consistent with the previous studies in different polymeric materials possessing banded spherulites. The handedness of spiral twists has been found to be unique only if the materials reveal specific chirality for their molecular entities.²⁹ Significant surface roughening with periodic thickness variation was observed so that a wavylike morphology was formed. These lamellar crystals display shallow curved C-shapes and S-shapes while the lamellae locate on the ridges of wavy spraying (Figure 7, parts b and c). Similar textures have been reported for etching results of numerous samples with the presence of banded spherulites. The origins of the C-shape and S-shape lamellae have been studied by Lustiger and co-workers through etching experiments and computer modeling in great detail.²⁸ It was also noted that the separated distance between these concentric rings in PLM and in TEM was not equivalent. Banded spherulites crystallized from thinner samples form smaller separations. This discrepancy reflects that the spacing of banded rings is indeed affected by the sample thickness.

Morphology of Single Crystals. Figure 8a shows the TEM micrograph of PTT samples crystallized from the melt at 225°C for more than 20 h. Banded spherulitic morphology can be still recognized while this thin film sample was observed by PLM after careful adjustment for brightness and focus. As usual, these

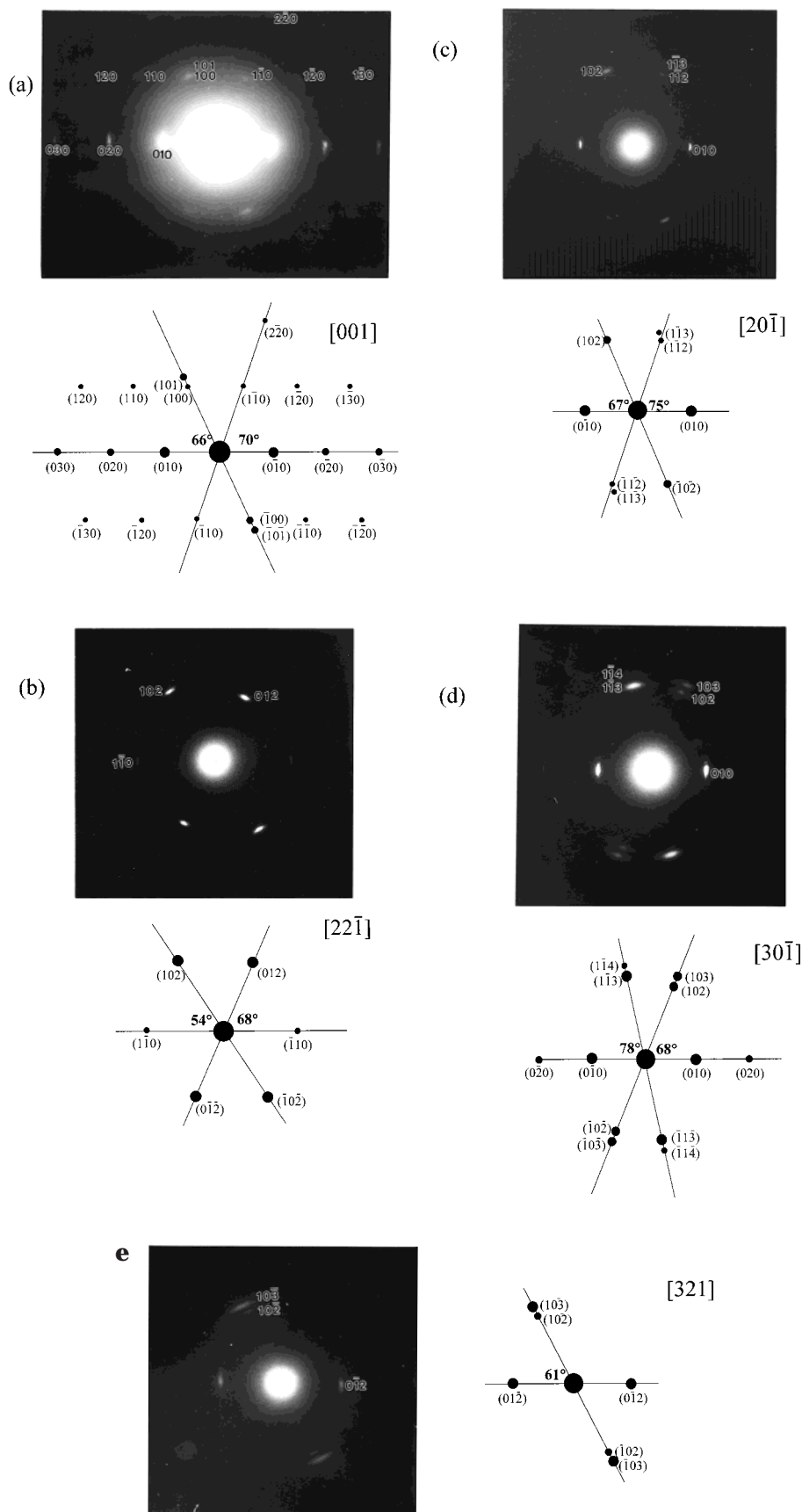


Figure 2. ED patterns for melt-crystallized PTT obtained from the single-crystal lamellae: (a) along the [001] zone; (b) along the [221] zone; (c) along the [201] zone; (d) along the [301] zone; (e) along the [321] zone.

lamellae spirally grow from the center of spherulites and form slightly wavylike morphology. However, a quite different situation was observed; these spherulites

consisted of large single crystal lamellae instead of lamellar fibrils. Single crystal ED patterns can be thus obtained from these crystals, in particular the lamellae

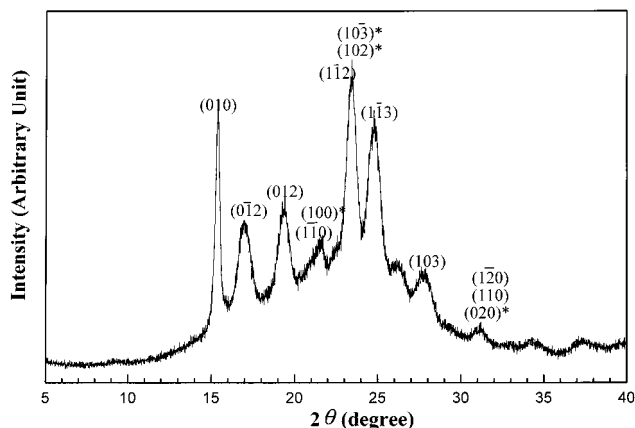
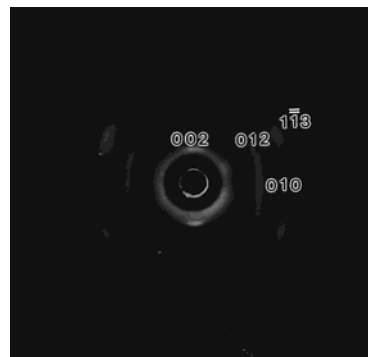
Table 1. Unit Cell Parameters of PTT (Comparison of WAXD and ED Experiments)

	fiber ^a WAXD	powder WAXD	ED
<i>a</i> (Å)	4.64	4.53	4.5
<i>b</i> (Å)	6.27	6.20	6.3
<i>c</i> (Å)	18.64	18.7	18.2
α (deg)	98.4	97.6	97.5
β (deg)	93.0	93.2	91.4
γ (deg)	111.1	110.1	111.7
density (g/cm ³)	1.387	1.408	1.44

^a From ref 4.**Table 2. Comparison of the Experimental and Calculated Interplanar Angles (deg) in ED Patterns**

zone	inter-plane	θ_{calcd}	θ_{exptl}	inter-plane	θ_{calcd}	θ_{exptl}
[001]	(010)(100)	67.9	66	(0 $\bar{1}$ 0)(1 $\bar{1}$ 0)	69.6	70
[2 $\bar{2}$ 1]	(1 $\bar{1}$ 0)(102)	50.4	54	(1 $\bar{1}$ 0)(012)	73.2	68
[20 $\bar{1}$]	(010)(112)	75.3	75	(0 $\bar{1}$ 0)(102)	66.9	67
[30 $\bar{1}$]	(010)(103)	67.6	68	(0 $\bar{1}$ 0)(1 $\bar{1}$ 3)	78.4	78
[32 $\bar{1}$]	(012)(103)	58.9	61			

located in the troughs of the wavylike morphology. An interesting observation can be further identified that the majority of single crystal ED patterns obtained from the trough area possesses same zonal axis. The ED pattern of [001] zone was easily found in these regions while the samples were tilted about 10° from the normal of the thin film surface. To realize the particular results, studies of spatial correlation between crystal lattice and reciprocal lattice were carried out based on the determined triclinic structure. An interesting coincidence was found where the angle between the *c* axis of crystal structure and the *c** axis of reciprocal lattice is 8.7°, which is approximately equal to the tilting angle of previous ED experiments. Different tilting stages were also performed to examine the observed morphology. On the basis of the spatial relationship between tilting angles and their corresponding diffraction results, we inferred that the basal plane of single crystals is the *ab* plane of PTT triclinic structure. The chain molecules were found to be inclined at about 10° to the normal of the basal plane. In accordance of the correlation of observed image and its selected area ED pattern (Figure 8a), we found that the reciprocal lattice vector of *a** exists with an explicit connection to the radial direction of the observed spherulite. Figure 8b exhibits the projection of the crystal *ab* plane onto the *a*b** plane of the reciprocal lattice. This observation indicated that the radial growth direction (i.e., the extended axis of the single crystal lamellae) corresponds approximately to the *a* axis direction of crystal structure. The growth planes of the crystal are thus implied as a (010) type. According to the observed results, the geometry of PTT single-crystal lamellae grown from the melt is illustrated in Figure 9a. This result of preferred growth direction is consistent with the morphological observations of PTT crystal lamellae grown from dilute solution.⁴ Two possible folding planes, (100) and (010) planes (i.e., *bc* and *ac* planes) of the crystal structure, may be assumed for the lamellar growth. According to recent studies by Cheng and co-workers, the folding plane has been identified as the (010) plane.³³ The inclination of chain stems for melt-crystallized lamellae is different from the reported flat-on disposition for solution-crystallized lamellae. The tilting of the folding plane to the lamellar normal has been found to be prerequisite for the formation of characteristic banded textures in PTT samples (see discussion section for reasons).

**Figure 3.** WAXD powder pattern for PTT crystallized at 225 °C from the melt. The asterisk (*) indicates the major reflection in the diffraction peak.**Figure 4.** WAXD fiber pattern for spun filaments of PTT from the melt.

Discussion

Stable Structure of PTT. Structure transformation of crystallizable polymers may occur while the polymers are stretched. In the range of small strain, the deformation process for crystallized polymeric materials is elastic and reversible so that the transformed structure reverses to its original dimensions after the removal of stress. The transformation of crystal structure may be permanent when the polymer is stretched beyond the yield point. For polymeric materials, the determination of crystal structure is usually carried out by WAXD fiber experiments due to the difficulties to obtain the diffraction patterns of single crystal. To obtain uniformly oriented fibers, samples are, in general, spun to a high draw ratio at which permanent deformation may form after drawing. The transformed structure is thus stabilized by residual stress after the removal of large extension. For ED experiments, the crystals for diffraction are grown directly from the melt or solution. Namely, the crystals are formed under strain-free condition.

In this study, large lamellar crystals were formed and unit cell parameters can be thus determined (Table 1). Corresponding to ED results, unit cell parameters identified by WAXD powder experiments were found to be rather close to parameters by ED experiments. The determined parameters were also consistent with the results from WAXD fiber pattern reported by Poulin-Dandurand and co-workers.⁴ The crystal density of PTT was also calculated according to its unit cell parameters. We have found that the crystal grown from the melt of thin film possesses the highest crystal density (1.44

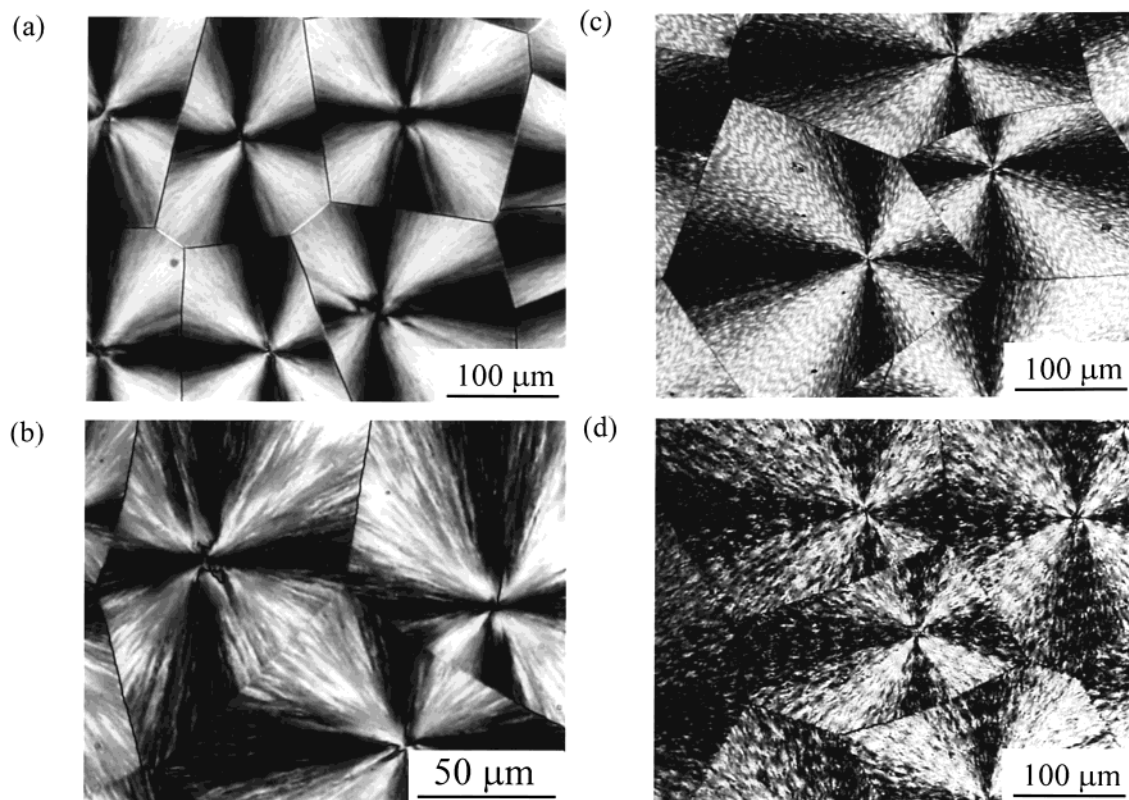


Figure 5. Transmitted PLM micrographs of PTT samples crystallized at different crystallization temperatures from the melt: (a) 185 °C; (b) 195 °C; (c) 205 °C; (d) 215 °C.

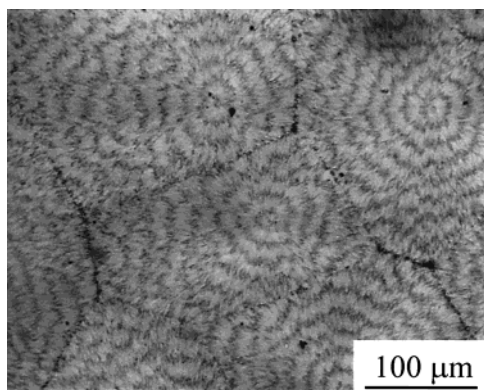


Figure 6. Reflected optical micrograph of PTT sample in Figure 5d.

g/cm^3) as compared to the bulk sample (1.404 g/cm^3) and fiber sample (1.387 g/cm^3). This result is consistent with the consequence of alleged strain-free crystals; the higher perfection of crystal is formed under a less disturbed environment. The comparison results also indicated that the PTT structure possesses close unit cell dimensions regardless of sample preparation. We speculate that the structure is easy to revert to its original dimensions after removal of stress. Since the fibers in Poulin-Dandurand's paper⁴ were annealed at high temperature after necking by extension, it is possible to relax them back after high-temperature annealing. To further confirm our speculation, spun fibers without any further annealing were prepared in this study. The dimension of c axis is calculated as 18.74 \AA that is almost equal to the determined dimension from WAXD powder pattern. For terephthalic polyesters, it is believed that unit cell parameters are dependent upon

the stressed conditions. In particular, a crystal structure transformation with significant dimensional change in c axis was observed for PBT samples after stretching. This transformation behavior of PBT is intrinsically different to the structural invariant of PTT after relaxation from stretching. It has been recognized that the 2/1 helical conformation of PTT possesses a larger flexibility to extend under stress. According to the behavior of the dimensional invariant, we speculate that the unique helical structure should possess a lower energy barrier for the rearrangement of the chain conformation. The lower energy barrier thus leads to a larger elongation under extension and easy relaxation after removal of stretching. Although further studies regarding the energy contour of conformation changes are necessary to clarify this behavior, the dimensional invariant may explain better performance in resilience recovery for PTT as compared to PET and PBT.

The Origins of Banded Spherulite. Usually, banded extinctions of spherulite in terephthalic polyesters, such as PET and PBT, are difficult to recognize by PLM due to dense nucleation for samples crystallized from thin films. The size of the banded spherulite is too small to be observed under the resolution of PLM unless the sample is sectioned from melt-crystallized bulk.²⁵ Unlike PET and PBT, the banded spherulites of PTT thin films can be distinctly observed since large spherulites are formed from the melt. This characteristic feature makes PTT a good candidate to study the origins of banded spherulites in terephthalic polyesters. In such a case, the correlation between the banded texture observed in transmitted PLM and the organization of lamellar stems can be visualized by transmission electron microscopy complemented with electron diffraction.

It is commonly believed that the periodic extinction of banded spherulite is led by lamellar twisting during

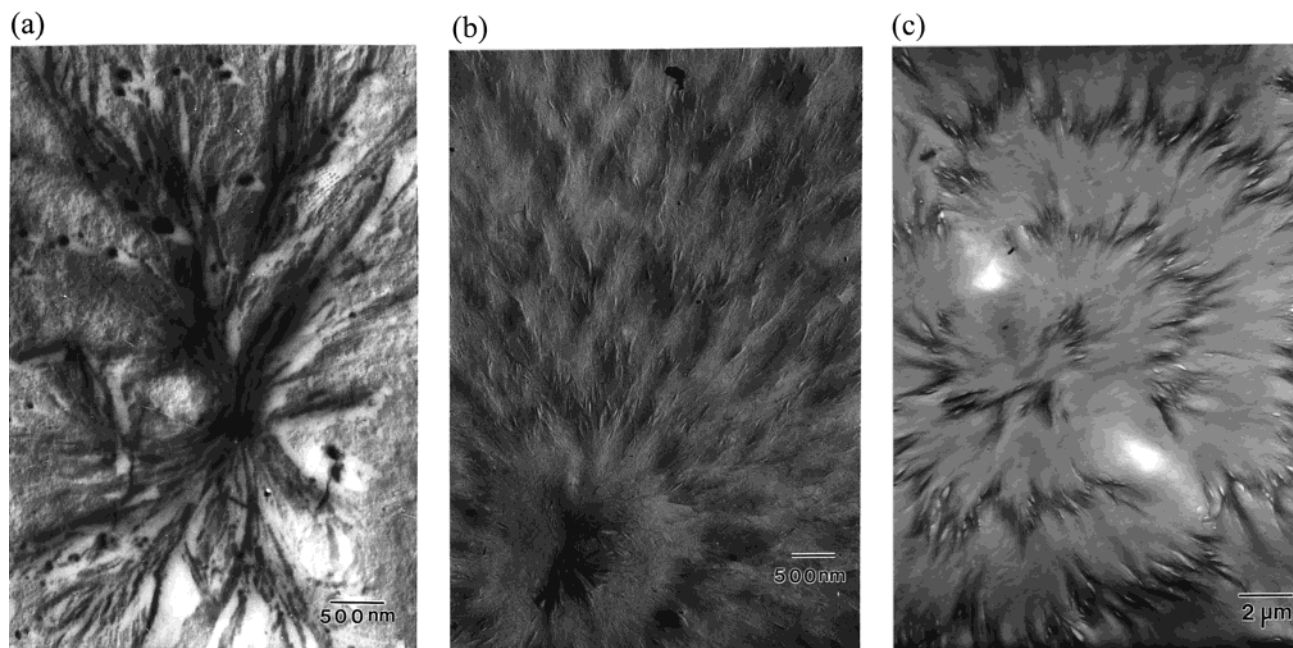


Figure 7. TEM micrographs of PTT samples crystallized at different crystallization temperatures from the melt: (a) 195 °C; (b) 205 °C; (c) 215 °C.

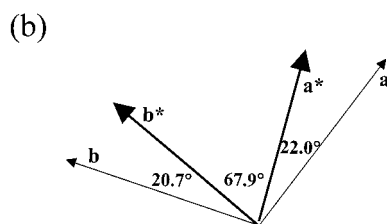
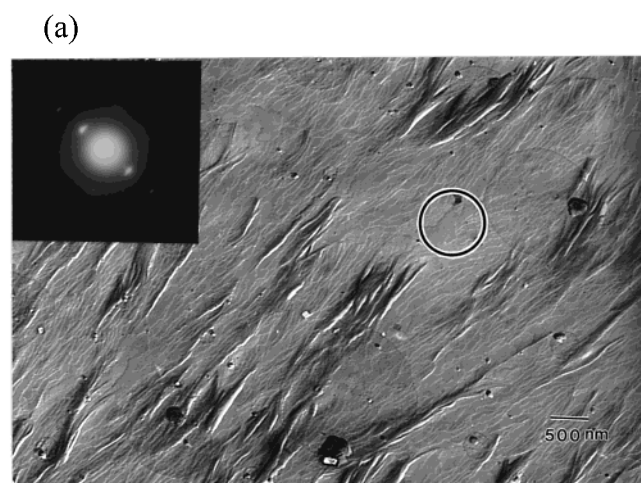


Figure 8. (a) TEM observation of PTT sample crystallized at 225 °C from the melt. The ED pattern is obtained from the circled area of the micrograph and shown in correct orientation. (b) Projection of the crystal ab plane onto the a^*b^* plane of the reciprocal lattice.

growth. Extinction takes place when the direction of rotative optical axis (i.e., the direction of molecular chains) is parallel to the transmitted light of PLM. In thin film samples with free surface, the unrestrained lamellae develop in twisted manner along the radial direction of spherulites so as to generate periodic thickness variation. In other words, alternating surface ridges and valleys (i.e., wavylike morphology) are formed after crystal growth. A plausible result was

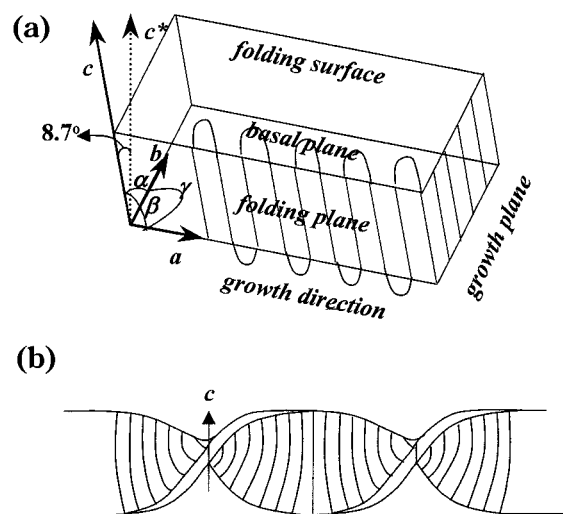


Figure 9. Schematic representation of (a) the lamellar geometry of PTT single crystal and (b) the twining mechanism of the intralamellar model in PTT.

obtained where the wavylike morphology of PTT was observed by reflected light microscopy (Figure 6), and it corresponded well to the periodic extinction of banded spherulites observed by PLM (Figure 5d). The dark regions of surface troughs in reflected light microscopy are matched with the regions of dark rings in PLM. This result clearly indicates that the formation of banded spherulites is attributed to the lamellar twisting along the spherulitic radials. Instead of surface replicas or staining for sections from bulk, thin film samples after shadowing of heavy metal were examined by TEM directly. As observed, wavylike morphology was also observed by TEM (Figure 8a). The shallow C-shaped and S-shaped textures in the crest regions are attributed to the shadowed effect of elevated portions raised by lamellar twisting. These results are consistent with proposed mechanism for the formation of C-shaped and S-shaped textures by Lustiger and co-workers.²⁸ They suggested that the special lamellar shapes are not

necessarily intrinsic to the lamellar profile but may arise due to geometrical effects as the lamellae project onto a surface at various angles. Thus, we speculate that the formation of incomplete C-shapes and S-shapes is caused by the thickness limitation of thin film sections so as to form incomplete helical rotation. This limitation, however, is beneficial to the studies of the correlation between banded texture and the organization of lamellar stems. Although continuous and cooperative twisting occurs, large lamellae with approximately uniform orientation are still formed due to mild bending. Deriving from their corresponding single-crystal ED patterns at different tilting stages and their related locations, the evolution of lamellar growth were thus identified. We found that the lamellae located on the trough regions formed near flat-on morphology (i.e., molecular chains of crystals are about 10° tilt to the normal of substrate surface), as shown in Figure 9a. Moreover, based on the results of tilting experiments, the lamellae form shallow C-shaped and S-shaped crests while they tend to form edge-on morphology (i.e., molecular chains of crystals are parallel to the substrate surface). The formation of alternating flat-to-edge-on morphology in TEM is in accordance with the appearance of alternating dark-to-bright rings in transmitted PLM as well as the wavylike morphology in reflected light microscopy. These observations are consistent with the previous findings that certain out-of-zone reflections with distinct l of Miller indices appeared where molecular chains continuously tilt from the lamellar normal, and thus bring the abnormal reflections.

On the basis of the geometry of single-crystal lamellae (Figure 9a), we suggest that the chain stems maintain a nonorthogonal relationship to the fold surfaces by canting toward the radial direction of the spherulite that is determined to be close the a axis direction. As suggested by Keith and Padden, different degrees of disorder develop at opposite fold surfaces giving rise to surface stresses, which result from the bending moments of chain tilting.²⁷ The induced surface stresses will cause the formation of predominantly helically twisted lamellae as shown in Figure 9b. Moreover, the molecular arrangement accommodated in this illustration indeed agrees with the appearance of negative birefringence where molecular stems are tangent to spherulitic radials.

Conclusion

After the growth of large single crystal from the melt, the unit cell parameters of PTT structure at strain-free condition were determined by ED experiments. They are $a = 4.5 \text{ \AA}$, $b = 6.3 \text{ \AA}$, $c = 18.2 \text{ \AA}$, $\alpha = 97.5^\circ$, $\beta = 91.4^\circ$, and $\gamma = 111.7^\circ$ with a calculated density of 1.44 g/cm^3 . Corresponding reflections in wide-angle X-ray diffraction powder pattern was thus identified and indexed. A much more precise determination of unit cell parameters was obtained. They are $a = 4.53 \text{ \AA}$, $b = 6.20 \text{ \AA}$, $c = 18.70 \text{ \AA}$, $\alpha = 97.6^\circ$, $\beta = 93.2^\circ$, and $\gamma = 110.1^\circ$. It is interesting to find that the change of unit cell parameters in PTT fiber is minor after removal of extension. We speculate that the easy rearrangement of PTT chains leads to better performance in resilience recovery.

A typical banded spherulite with negative birefringence was observed in PTT. After the observations of wavylike morphology, we suggest that the appearance

of banded spherulites results from lamellar twisting which generates alternating flat-to-edge-on morphology. In this study, the geometry of crystal lamellae was well defined after the analysis of lamellar morphology and its correlated single-crystal ED patterns. The PTT lamellae grow from the basal plane consisting of a and b axes, and the chain stems uphold a nonorthogonal relationship to the fold surfaces by canting toward the radial direction of the spherulite. As a result, surface stress resulting from the folding surface is gradually accumulated so as to drive the crystal twist. The twisting is attributed to an intralamellar origin to the lamellar geometry. It should be noted that numerous materials appear the morphology of banded spherulites, and different mechanisms have been proposed to interpret various systems. It is not necessary to have a nonorthogonal relationship for the formation of banded extinction. The value of this study is to give an explanation for the origins of banded spherulites in terephthalic polyesters based on the detailed analysis of the shape and organization of the lamellar in the banded spherulites.

Acknowledgment. The authors would like to thanks Dr. Stephen Z. D. Cheng and Mr. Anquin Zhang at Institute of Polymer Science of University of Akron for their helpful discussion. We also wish to thank Mr. I-Min Tseng at Industrial Technology Research Institute of Taiwan for supplying the polymers used in this study. The financial support of the National Science Council (Grant NSC89-2216-E110-006) is acknowledged. R.M.H. would also like to thank Ms. S.-Y. Lee of Regional Instruments Center at NSYSU and Ms. P.-C. Chao at NCHU for their help in the WAXD and ED experiments, respectively.

References and Notes

- (1) Traub, H. L. *Angew. Makromol. Chem.* **1995**, 179, 4055.
- (2) Goodman, I. *Angew. Chem.* **1962**, 74, 606.
- (3) Jakeways, R.; Ward, I. M.; Wilding, M. A.; Hall, I. H.; Desborough, I. J.; Pass, M. G. *J. Polym. Sci., Polym. Phys. Ed.* **1975**, 13, 799.
- (4) Poulin-Dandurand, S.; Perez, S.; Revol, J.-F.; Brisse, F. *Polymer* **1979**, 20, 419.
- (5) Sun, T.; Zhang, A.; Li, F. M.; Porter, R. S. *Polymer* **1988**, 29, 2115.
- (6) Zhang, A.; Jiang, H.; Wu, Z.; Wu, C.; Qian, B. *J. Appl. Polym. Sci.* **1991**, 42, 1779.
- (7) Fu, Y.; Busing, R.; Jin, Y.; Affholter, K. A.; Wunderlich, B. *Macromolecules* **1993**, 26, 2187.
- (8) Liu, J.; Geil, P. H. *J. Macromol. Sci. Phys.* **1997**, 36, 61.
- (9) Yokouchi, M.; Sakakibara, Y.; Vhatani, Y.; Tadokoro, H.; Tanaka, T.; Yado, K. *Macromolecules* **1976**, 9, 266.
- (10) Hall, I. H.; Pass, M. G. *Polymer* **1976**, 17, 807.
- (11) Liu, J.; Geil, P. H. *J. Macromol. Sci. Phys.* **1997**, 36, 263.
- (12) Hall, I. H.; Pass, M. G.; Rammo, N. N. *J. Polym. Sci., Polym. Phys. Ed.* **1978**, 16, 1409.
- (13) Hall, I. H.; Rammo, N. N. *J. Polym. Sci., Polym. Phys. Ed.* **1978**, 16, 2189.
- (14) Keller, A. *J. Polym. Sci.* **1955**, 17, 351.
- (15) Keith, H. D.; Padden, F. J., Jr. *J. Polym. Sci.* **1959**, 39, 101.
- (16) Keith, H. D.; Padden, F. J., Jr. *J. Polym. Sci.* **1959**, 39, 123.
- (17) Price, F. P. *J. Polym. Sci.* **1959**, 39, 139.
- (18) Keller, A. *J. Polym. Sci.* **1959**, 39, 151.
- (19) Fujiwara, Y. *J. Appl. Polym. Sci.* **1960**, 4, 10.
- (20) Schultz, J. M.; Kinloch, D. R. *Polymer* **1969**, 10, 271.
- (21) Bassett, D. C.; Hodge, A. M. *Polymer* **1978**, 19, 469.
- (22) Bassett, D. C.; Hodge, A. M. *Proc. R. Soc. London, Ser. A* **1981**, 377, 61.
- (23) Bassett, D. C.; Vaughan, A. S. *Polymer* **1985**, 26, 717.
- (24) Bassett, D. C.; Olley, R. H.; Al-Raheil, A. M. *Polymer* **1988**, 29, 1539.
- (25) Keller, J. *J. Polym. Sci.* **1955**, 17, 291.

- (26) Hoffman, J. D.; Lauritzen, J. I. *J. Res. Natl. Bur. Stand. USA* **1961**, 65A, 297.
- (27) Keith, H. D.; Padden, F. J., Jr. *Polymer* **1984**, 25, 28.
- (28) Lustiger, A.; Lotz, B.; Duff, T. S. *J. Polym. Sci. Polym. Phys. Ed.* **1989**, 27, 561.
- (29) Singfield, K. L.; Klass, J. M.; Brown, G. R. *Macromolecules* **1995**, 28, 8006.
- (30) Geil, P. H. In *Polymer Single Crystals*; Mark, H. F., Immergut, E. H., Eds.; John Wiley & Sons: New York, 1963.
- (31) Li, C. Y.; Cheng, S. Z. D.; Ge, J. J.; Bai, F.; Zhang, J. Z.; Yan, D.; He, T.; Chien, L.-C.; Harris, F. W.; Lotz, B. *Phys. Rev. Lett.* **1999**, 83, 4558.
- (32) Li, C. Y.; Cheng, S. Z. D.; Ge, J. J.; Bai, F.; Zhang, J. Z.; Mann, I. K.; Chien, L.-C.; Harris, F. W.; Lotz, B. *J. Am. Chem. Soc.* **2000**, 122, 72.
- (33) Cheng, S. Z. D. Personal communication.

MA000210W